Available online at www.sciencedirect.com
ScienceDirect
Journal of Molecular Graphics and Modelling 26 (2007) 457–470
Journal of Molecular Graphics and Modelling
www.elsevier.com/locate/JMGM

Insights into ligand selectivity in nitric oxide synthase isoforms: A molecular dynamics study

V. Aparna [a], G.R. Desiraju [a,*], B. Gopalakrishnan [b,**]

[a] School of Chemistry, University of Hyderabad, Hyderabad 500046, India
[b] Life Sciences R&D Division, Advanced Technology Centre, TATA Consultancy Services Limited, 1 Software Units Layout, Madhapur, Hyderabad 500081, India

Received 25 September 2006; received in revised form 12 February 2007; accepted 12 February 2007
Available online 15 February 2007

Abstract

Molecular dynamics (MD) simulations were carried out for inducible nitric oxide synthase (iNOS) and endothelial nitric oxide synthase (eNOS) isoforms complexed with substrate (L-arginine) and the iNOS specific inhibitor GW 273629, **2** for a time period of 1.2 ns. The simulations were compared both within and across the isoforms. iNOS specificity of inhibitor **2** is attributed to water mediated interactions and cooperative hydrogen bond networks. Juxtaposition of the carboxylic and ammonium groups in the substrate and inhibitor serve as a modulating key in binding to the isoforms. Based on these investigations, molecules **3** and **4** were rationally designed to attain specificity among the isoforms. The capability of the designed ligands was theoretically tested through MD simulations to envisage binding patterns with both isoforms. A detailed analysis of the molecular recognition pattern shows molecule **4** to be more selective to iNOS when compared to eNOS.

Keywords: Nitric oxide synthase; Molecular dynamics; Isoform selectivity; Water

1. Introduction

Nitric oxide synthase (NOS) catalyzes the oxidation of L-arginine to nitric oxide (NO) and L-citrulline [1]. It is expressed as three isoforms: constitutive endothelial NOS (eNOS), neuronal NOS (nNOS), and cytokine inducible NOS (iNOS) isoforms. The isoforms share a common architecture of the N-terminal oxygenase domain and the C-terminal reductase domain connected by a calmodulin (CaM) binding linker. The oxygenase domain binds heme, tetrahydrobiopterin (H_4B) and the substrate, L-arginine as shown in Fig. 1, while the reductase domain binds to FAD, FMN, and NADPH cofactors. While the oxygenase domain provides the site for catalysis, the FAD and FMN of the reductase domain transfer the electrons required for catalysis. Constitutive eNOS and nNOS generate low levels of NO that is imperative for blood circulation and signal transmission in the nervous system, respectively [2]. The activity of these constitutive enzymes is regulated at the post translational level, through Ca^{2+} dependent CaM binding [3]. On the other hand, iNOS is expressed upon activation by various pro-inflammatory agents like endotoxin, interleukin-12 and other cytokines. Once expressed, iNOS produces high levels of NO over long periods of time, as a host defense mechanism.

Generation of NO propagates through a two-step oxidation from L-arginine to L-citrulline [4]. The reaction proceeds through a stable intermediate, N^{ω}-hydroxy-L-arginine (NHA) as shown in Scheme 1. The first step involves hydroxylation of guanidinium nitrogen to form NHA, a mixed-function oxidation similar to those catalyzed by the cytochrome P-450. It includes sequential transfer of one electron from NADPH → FAD → FMN → heme to form a heme–oxygen complex, while H_4B provides the other electron for the formation of heme–peroxy complex [5–7]. In the second step NHA is oxidized to L-citrulline and NO radical.

Excessive production of NO generated either by iNOS, or by the sustained activation of nNOS, elicits cellular toxicity and tissue damage leading to various pathological conditions. Overexpression of iNOS derived NO is implicated in diseases like immune type diabetes, inflammatory bowel disease, rheumatoid arthritis, carcinogenesis, multiple sclerosis, transplant

* Corresponding author. Tel.: +91 40 55673591; fax: +91 40 55672222.
** Corresponding author. Tel.: +91 40 23134828; fax: +91 40 23010567.
E-mail addresses: gautam_desiraju@yahoo.com (G.R. Desiraju), gopal@atc.tcs.com (B. Gopalakrishnan).

1093-3263/$ – see front matter © 2007 Elsevier Inc. All rights reserved.
doi:10.1016/j.jmgm.2007.02.003

Fig. 1. The oxygenase domain of eNOS with heme (pink), L-arginine (purple) and H_4B (green) in the active site.

rejection, and septic shock [8]. On the other hand, overproduction of NO by nNOS is linked to the pathogenesis of stroke, Alzheimer's, Parkinsons's, and Huntington's diseases. However, NO generated from eNOS is shown to be critical for angiogenesis and for maintaining the vascular tone. Also, the role of eNOS derived NO in maintaining the blood circulation is well implicated with the use of NO donating compounds as antihypertensives. Therefore, isoform specific inhibitors are desirable to specifically inhibit NO production by iNOS and nNOS under pathological conditions without inhibiting the functions of eNOS.

A number of substrate based analogs like N^{ω}-methyl-L-arginine methyl ester (L-NMMA), N^{ω}-nitro-L-arginine (L-NNA), N^{δ}-iminoethyl-L-orthinine (L-NIO), L-N^{6}-(1-iminoethyl)lysine [9], and non-amino acid analogues like iminopiperidines [10], quinazolinamines [11], aminoguanidines, isothioureas, carbamidines have been developed. However, these ligands show minimal selectivity towards the isoforms. Very few molecules are known to show selective inhibition of NOS isoforms, and the basis of their selectivity remains unknown. Several crystal structures of human iNOS and eNOS isoforms with various classes of inhibitors have been determined [12–16]. This has helped to identify the structural variations and their implication in the design of selective inhibitors. NOS isoforms share a common topology, with a striking degree of conservation in the active site. The oxygenase domains of iNOS and eNOS structures have 57% sequence identity over 435 residues. The RMSD of the backbone atoms between iNOS and eNOS oxygenase domains is 0.714 Å. The active site of the isoforms is highly conserved with only one residue differing (Asp382 in iNOS mutated to Asn366 in eNOS) among those forming direct contacts with the substrate. Fischmann et al. have proposed that use of larger competitive inhibitors that extend out of the binding site can exploit this key active site difference to yield isoform specific inhibitors [15].

The high structural similarity between the active sites of the isoforms presents a challenging problem for the design of selective inhibitors [15]. To circumvent these problems it is essential to critically examine the structural differences in the active site among different isoforms and to understand how the known isoform selective inhibitors interact with their active sites. In this context, the substrate L-arginine (**1**) and GW273629 {(2S)-2-amino-3-[2-(1-iminoethylamino)ethylsulfonyl]propanoic acid} (**2**), a selective iNOS inhibitor with IC_{50} values of 8 μM and >1000 μM for iNOS and eNOS, respectively [17], were selected for the present study. Understanding the structural and dynamical features of binding of molecule **2** with these isoforms is expected to further increase our insights towards its selectivity and aid in the development of selective and potent inhibitors of the two isoforms. With this perspective, the molecular recognition pattern of the substrate and inhibitor, **2** was thoroughly explored in iNOS and eNOS isoforms. Based on these investigations, active site differences were exploited to bring in selectivity to the isoforms. To accomplish this, molecular dynamics (MD) simulations were carried out with isoforms iNOS and eNOS complexed with substrate (**1**), GW273629 (**2**) and two designed ligands **3** and **4** as shown in Fig. 2.

2. Methodology

2.1. Initial structure preparation

The crystal structures of iNOS [18] and eNOS [15] isoforms complexed with L-NHA and L-arginine, respectively, were taken from the protein data bank [pdb code 1NSI (iNOS); 3NOS (eNOS)]. The isoform exists as a dimer with structural Zn^{2+} ion coordinating with the four cysteines, two cysteines from each monomer: Cys110 and Cys115 of each monomer in

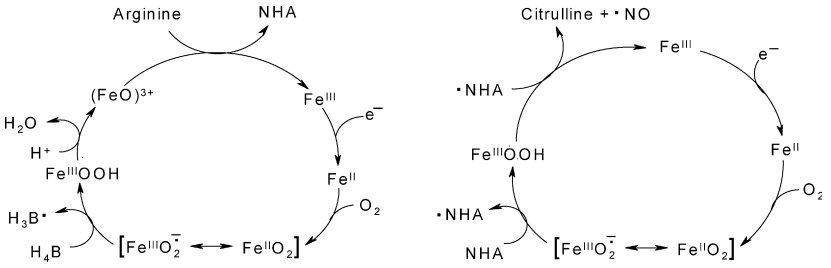

Scheme 1. Mechanism of NO production in NOS.

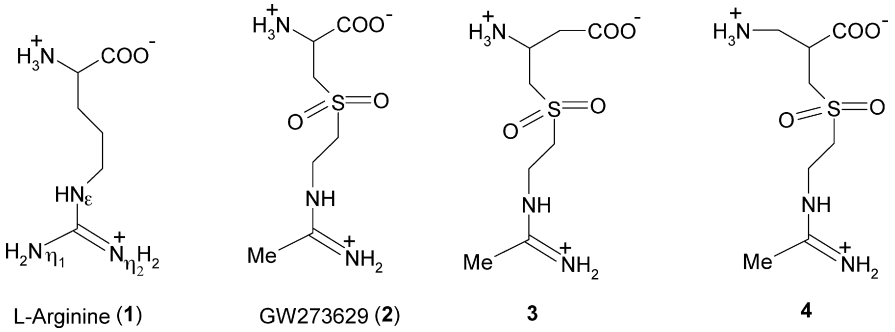

Fig. 2. Ligands used in the MD simulations.

iNOS (Cys95 and Cys99 in eNOS). The Zn^{2+} ion was excluded from the simulation because (i) it is situated ~22 Å away from the substrate bound site and has no effect on the substrate binding. (ii) Li et al. have shown experimentally that in the absence of Zn^{2+} ion, the symmetry related cysteines form a disulfide bridge [18]. Only monomer of each isoform (with 425 and 404 residues in iNOS and eNOS, respectively) was used in the study. H-atoms were added to the complex at pH 7 using the biopolymer module in the *Insight II* program [19]. The His residues 102, 162, 230, 333, 436, 477, 499 in iNOS and residues 214, 420, 421, and 461 in eNOS were designated as the ε-tautomers, while the rest were designated as δ-tautomers based on their hydrogen bonding preferences. Force field charges were applied while assigning a charge of +3 on the Fe atom of heme. The complex was minimized using steepest descent and conjugate gradient algorithms with a convergence criteria of 0.1 and 0.01 kcal mol^{-1} $Å^{-1}$, respectively. The energy minimization and MD simulations were performed with 'extensible systematic force field' (ESFF) [20] in the *Discover* module of *Insight II*. All the other ligands used in the simulation (Fig. 2) were constructed and energy minimized using the OFF methods module in *Cerius*^{2} [21]. Geometry optimization was carried out with the MOPAC 6 package using the semi-empirical AM1 Hamiltonian.

2.2. Molecular docking

All the four ligands in the study were docked into the structures of iNOS and eNOS enzymes. Docking was carried out using GOLD [22], which uses the genetic algorithm (GA). For each of the 10 independent GA runs, a maximum number of 100,000 GA operations were performed on a set of 5 groups with a population size of 100 individuals. Operator weights for crossover, mutation, and migration were set to 95, 95, and 10, respectively. Default cut-off values of 2.5 Å (d_{H-X}) for hydrogen bonds and 4.0 Å for non-bonded interactions were employed. When the top three solutions attained RMSD values within 1.5 Å, docking was terminated. The best ranked solution of the ligands was used for the MD simulations.

2.3. Molecular dynamics

To study the structural and dynamical properties of the protein, restricted MD simulations of each isoform were performed with the substrate and the inhibitor. The oxygenase domain of NOS is seen to be rigid with an exposed active site. A series of inhibitors co-crystallized with NOS show that the conformational changes in the isoform are confined to side chains of the active site residues [16]. The β strand architecture of the active site has been implicated to impart rigidity to the NOS structure [23]. Considering these facts, the simulations were confined to all the protein residues that contain at least one atom within 10 Å sphere from any atom of the ligand to reduce the computation time. Incidentally, this includes all the residues lining the substrate access channel (extending about 15 Å from the ligand). All the protein–ligand complexes were built in the *Biopolymer* module using the best docking solution obtained from GOLD. The complexes were explicitly solvated using the TIP3P [24] water model. The thickness of the hydration layer was selected to be 4 Å (from the surface of the protein) such that the total number of atoms in the complex did not exceed 10,000 atoms (limitation of ESFF [20]). This resulted in about 1250 water molecules in each system. The crystallographic waters and the water molecules added in the simulation were differentiated by adding 'H' and 'w' in their nomenclature, respectively. Force field charges were used for the protein complexes including water. Non-bonded interactions were calculated with a cut-off radius of 12 Å. Initially, water molecules were equilibrated with the system for about 50 ps while keeping all the protein heavy atoms fixed. All the simulations were carried out at room temperature, 300 K, with the temperature controlled by a Nosé-Hoover chain thermostat [25]. The simulations were carried out for 1.2 ns with NVT ensemble and a time step of 1fs. Newton's equations of motion were calculated using the velocity verlet algorithm. All the complexes were equilibrated for 200 ps and the trajectory was collected at each ps for 1 ns. The non-bonded interaction energies between the ligands and the active site residues were calculated using *Discover* module in *Insight II*.

3. Results and discussion

3.1. Overall structural changes

The analysis of the MD simulations for the fully solvated complexes of iNOS and eNOS with substrate (**1**), known inhibitor GW263729 (**2**), and the two hypothetical ligands **3** and **4** is now discussed. The potential energy of the system is a

simple measure of its stability. Plots of the potential energy as a function of time are shown in Fig. 3a, which indicate that all the systems in the study were well equilibrated and remain stable throughout the simulation. The stability of each protein complex during the simulation has also been monitored by plotting the RMSD of the complexes with respect to their initial structures as shown in Fig. 3b. The RMSD of the iNOS and eNOS complexes converged with mean values of 0.75 Å and 1.5 Å, respectively, which are within acceptable limits. The higher RMSD values of eNOS complexes depicts that eNOS has structural instability on binding with all the ligands when compared to iNOS. This is also confirmed by the plot of B-factor values in these isoforms (see Fig. 3c). The average hydrogen bond distances of all the interactions between the molecules **1–4** with the active site residues of iNOS and eNOS are given in Tables 1 and 2, respectively.

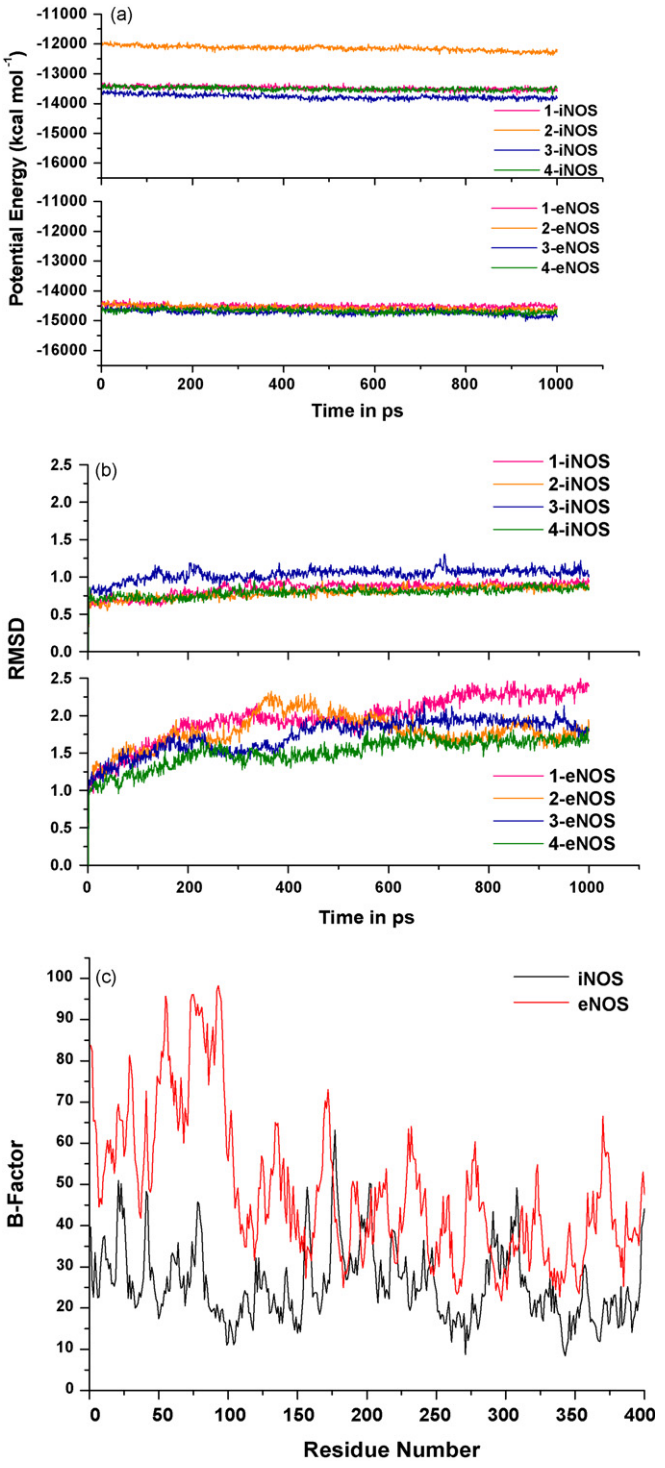

Fig. 3. Plots of (a) potential energy and (b) RMSD from initial structures of ligand complexes and (c) crystallographic B-factors of iNOS and eNOS isoforms.

Table 1
Average hydrogen bond distances between active site residues and ligands **1–4** in iNOS

Active site residues	**1**	**2**	**3**	**4**
Glu377	1.63 ± 0.08 1.59 ± 0.07	1.56 ± 0.06 1.67 ± 0.14	1.57 ± 0.07 1.58 ± 0.07	1.58 ± 0.06 1.60 ± 0.08
Glu377	–	2.71 ± 0.98	2.05 ± 0.44	–
Trp372	1.67 ± 0.09	1.70 ± 0.11	1.68 ± 0.11	1.75 ± 0.15
Tyr373	1.78 ± 013	–	–	–
Asp382	–	1.96 ± 0.63	2.08 ± 0.38	–
Arg266	1.63 ± 0.08	2.30 ± 0.34	2.24 ± 0.92	2.76 ± 0.75
Gln263	3.45 ± 0.56	1.80 ± 0.12	3.00 ± 0.37	–
Heme	1.89 ± 0.26	–	–	2.78 ± 0.20
Arg388	–	2.06 ± 0.39	2.41 ± 0.76	2.68 ± 0.83
H_4B	–	–	–	2.19 ± 0.69

3.2. Mode of substrate binding in iNOS and eNOS isoforms

The substrate, L-Arg (**1**) was docked into the active site of eNOS. The RMSD between the docked pose of **1** and its bound conformation in the crystal structure (3NOS) is 0.47 Å, indicating that GOLD was able to reproduce the correct pose. Therefore, all the ligands were docked using the same procedure. The detailed interactions of **1** with the active site residues of iNOS and eNOS are shown in Fig. 4. All the residues corresponding to eNOS are given in parentheses in this section for ease of comparison. The substrate consists of three functional groups: the ammonium and the carboxylate groups in the head region and the guanidinium group in the tail

Table 2
Average hydrogen bond distances between active site residues and the ligands **1–4** in eNOS

Active site residues	**1**	**2**	**3**	**4**
Glu361	1.86 ± 0.23 1.87 ± 0.16	1.61 ± 0.08 1.63 ± 0.09	1.59 ± 0.09 1.60 ± 0.08	1.60 ± 0.07 1.64 ± 0.09
Glu361	1.63 ± 0.23	–	–	–
Trp356	1.93 ± 0.19	1.65 ± 0.10	1.64 ± 0.08	1.66 ± 0.10
Tyr357	1.88 ± 0.19	1.71 ± 0.10	3.09 ± 1.57	1.76 ± 0.20
Asn366	1.89 ± 0.17	2.04 ± 0.27	2.60 ± 0.83	2.57 ± 0.65
Gln247	1.99 ± 0.28	1.95 ± 0.20	2.00 ± 0.36	3.17 ± 0.69
Arg250	3.15 ± 0.16	2.18 ± 0.68	2.19 ± 0.63	1.81 ± 0.29
Heme	1.74 ± 0.24	2.42 ± 0.69	1.60 ± 0.09	–
Arg372	–	1.75 ± 0.18	–	–
Tyr331	–	–	–	2.37 ± 0.69

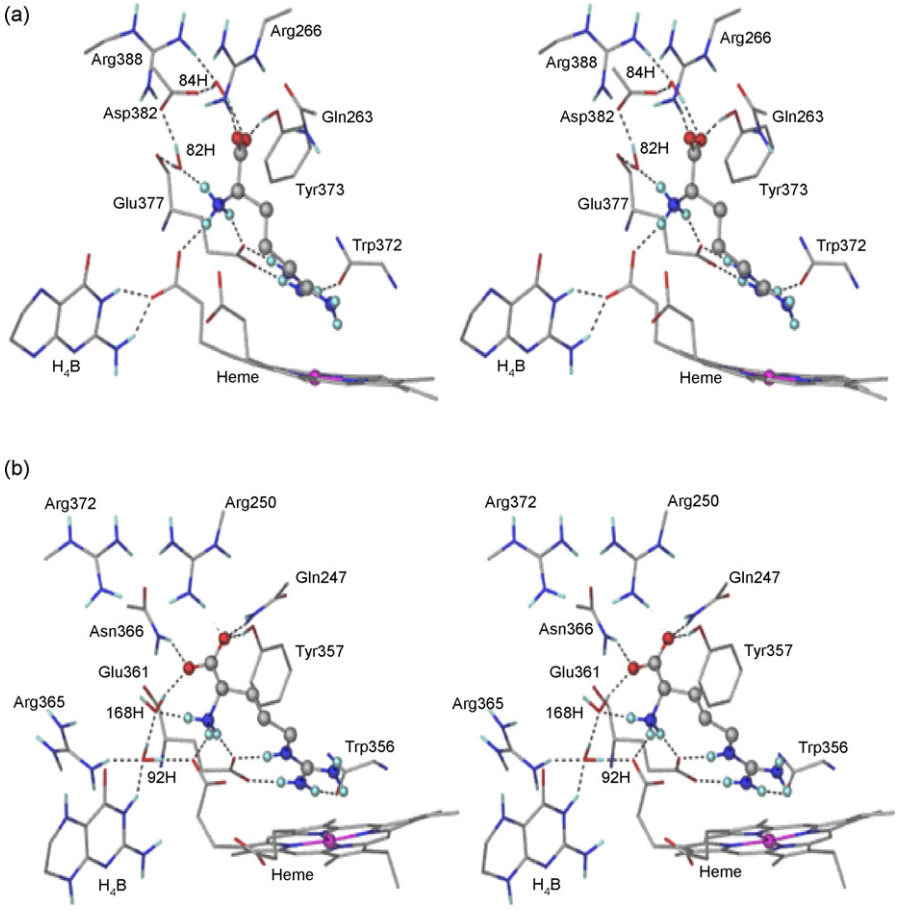

Fig. 4. Stereoview of active site of the (a) **1**–**iNOS** and (b) **1**–**eNOS** complexes. Molecule **1** (L-Arg) is shown in ball-and-stick representation. Hydrogen bonds are shown as dotted lines. Only selected H-atoms are shown for clarity.

region. The tail region of the substrate is anchored in the active site through a bidentate interaction between the guanidinium nitrogen atoms (Nε, $N\eta_1$) and the side chain carboxylate O-atoms of the Glu377 (Glu361) as seen in Fig. 4a. The importance of this residue has been revealed by site-directed mutagenesis studies where substitution of Glu by Gln, Leu or Ala resulted in loss of activity [26]. Additionally, the $N\eta_1$ atom of the substrate hydrogen bonds to the backbone carbonyl of Trp372 (Trp356). These interactions bring the guanidinium $N\eta_2$ atom of the substrate closer to the Fe of heme (3.6 Å in iNOS and 4 Å in eNOS). The close proximity of the heme iron to the $N\eta_2$ atom is consistent with the catalysis models of NOS [27]. The guanidinyl group stacks over the heme *meso* carbon and the edge of pyrrole ring A with an angle of ∼25° to the heme plane. The hydrogen bonds between the guanidinium group and the carboxylate of Glu377 (Glu361) are relatively short (see Table 1) due to charge assisted nature of hydrogen bonds. This has also been observed by Li et al. who reasoned that such short interactions were necessary to accommodate NO binding to Fe of heme during catalysis [28].

The binding conformation was also stabilized by hydrogen bonds formed by the ammonium and the carboxylate groups of the substrate in the head region: these groups seem to modulate the differences in molecular recognition of the substrate in the two isoforms. In both **1**–**iNOS** and **1**–**eNOS** complexes, the ammonium group of the substrate form hydrogen bonds with the water 82H (168H) [H corresponds to the crystal water], the heme carboxylate of pyrrole ring A and the side chain carboxyl $O\varepsilon_1$-atom of Glu377 (Glu361). Although the interacting residues are common in both the complexes, they differ in the entropy associated with these interactions. In iNOS, the interactions of the ammonium H-atoms interchange with the three acceptors viz., water 82H, heme and Glu377. Plots of the distances between the acceptor and the H-atoms of the ammonium group with time showed that these hydrogen bonds were retained throughout the simulation (Fig. 5a). The flipping of the three H-atoms of the ammonium nitrogen to form uninterrupted hydrogen bonds can be seen clearly. However, no such flipping was observed in the **1**–**eNOS** complex (Fig. 5b). The word entropy is used to refer the flipping of the ammonium hydrogens of the ligand as seen above. Grant et al. observed experimentally that the hydrogen bond between ammonium group of the substrate/inhibitor and the enzyme is essential for the catalysis and the absence of ammonium group in the ligand leads to loss of inhibitor activity [29]. However, their study limited the observation to iNOS and did not show details of the hydrogen bonds in the isoform. Further in the **1**–**iNOS**, water 82H was seen to mediate hydrogen bond interaction with Asp382, whereas in the **1**–**eNOS** complex no such interaction

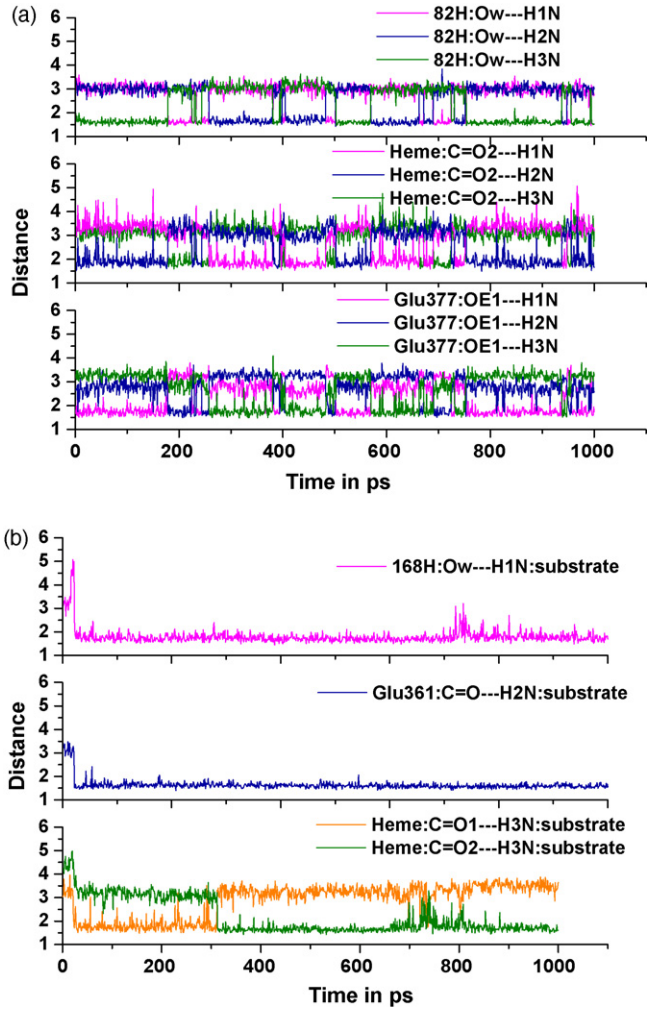

Fig. 5. Interactions between the ammonium group of the substrate **1** and the active site residues in the (a) **1–iNOS** and (b) **1–eNOS** complex. The interchanging of the three ammonium hydrogen atoms among the acceptors can be seen in (a).

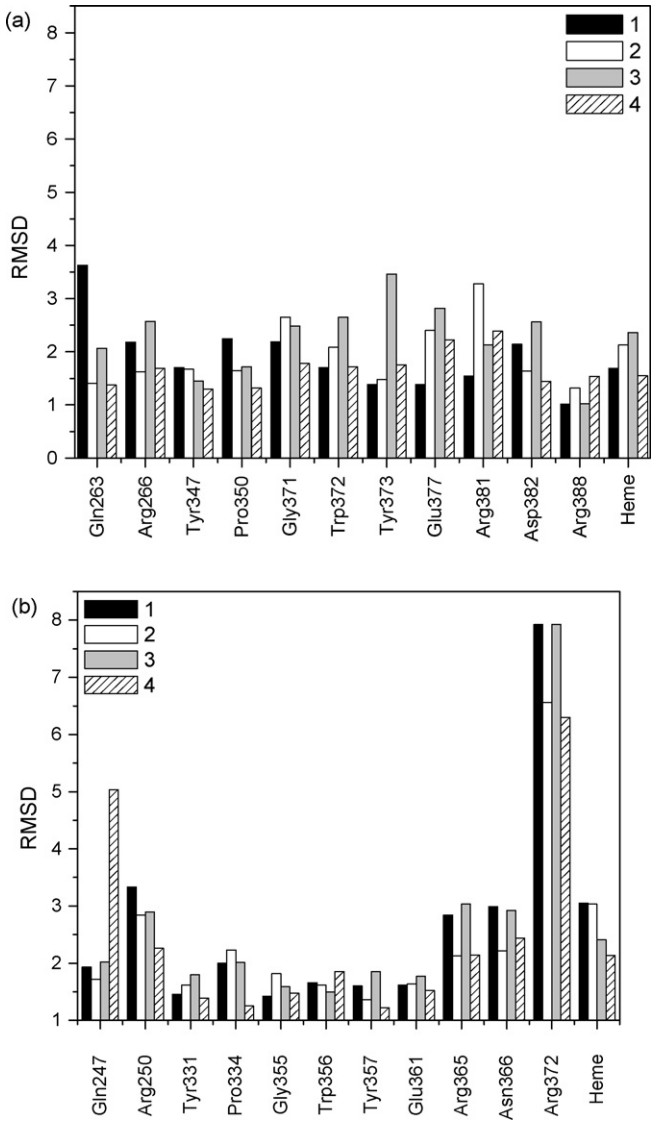

Fig. 6. RMSD of active site residues from its initial structure in (a) iNOS and (b) eNOS complexes.

was seen between the ammonium group and the corresponding residue Asn366.

In **1–iNOS**, the carboxylate group of the substrate forms hydrogen bonds with water 84H, Tyr373 and Arg266 (Fig. 4a). Although an interaction with Gln263 was also seen in the crystal structure, it was not retained throughout the MD simulation. In the **1–eNOS** complex, the carboxylate of the substrate interacts with water 168H, Tyr357, Asn366, and Gln247 (Fig. 4b). The electrostatic interaction with Arg250 (corresponding to Arg266 in iNOS) is absent in the **1–eNOS** complex. Fig. 6 shows the corresponding changes in the RMSD of the residues. Interestingly, water 168H binds to both the carboxylate and the ammonium groups of the substrate. This could be one of the reasons why flipping of the ammonium hydrogens is not observed with the **1–eNOS** complex. In addition to the enthalpic contribution, an entropic advantage due to the ammonium group in the **1–iNOS** complex provides extra stabilization when compared to **1–eNOS** complex. Apart from these interactions, van der Waals contacts were observed between the aliphatic chain of the substrate and the residues Pro350 (334), Val352 (336), and the alkyl chain of the heme propionate.

3.3. Differences in substrate recognition in the isoforms

The major difference in substrate recognition among the isoforms is the interaction with Asp382 (Asn366). While the ammonium group of the substrate participates in this recognition event through water mediation in iNOS, the carboxylate group interacts directly with the corresponding residue, Asn366 in eNOS. In comparison, substrate in eNOS rotates ~80° about C_α–COO^- bond to interact with the amide group of Asn366. Because of electrostatic repulsion between the carboxylate groups of Asp382 and the substrate in iNOS, the carboxylate group of the substrate moves away allowing the ammonium group to make water mediated interaction with Asp382. The juxtaposition of both the ammonium and the carboxylate groups in the substrate makes this variation feasible in both isoforms.

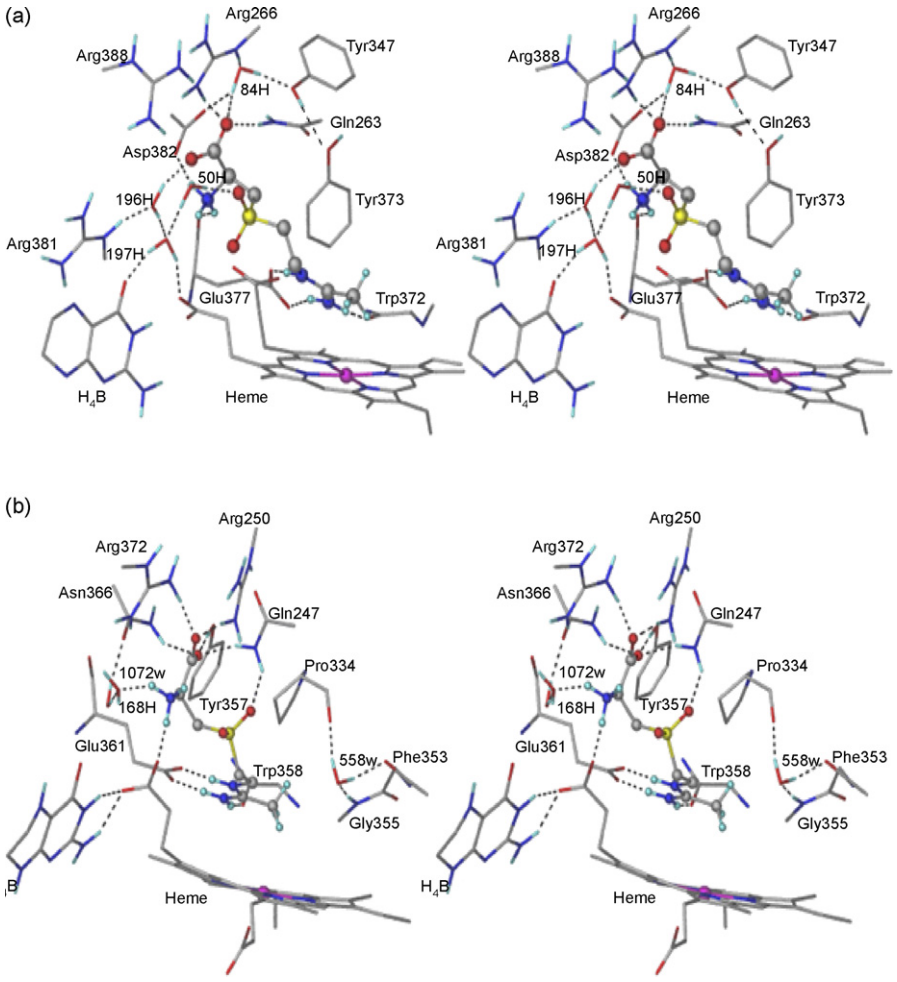

Fig. 7. Stereoview of the active site of the (a) **2–iNOS** and (b) **2–eNOS** complexes. Molecule **2** is shown in ball-and-stick representation.

3.3.1. Role of water in substrate binding

Water molecules trapped at the binding interface ostensibly constitute an unfavourable event owing to the entropic penalty. Conversely, water can contribute to the free energy of binding if the entropic loss is compensated by the enthalpic gain by forming (maximum number of) hydrogen bonds [30]. Two such water molecules are trapped at the interface of the **1–iNOS** complex, namely 82H and 84H. Each of these water molecules forms three hydrogen bonds with the active site residues. Water 82H mediates an interaction between the ammonium group of the substrate and the side chain carboxylate O-atom of Asp382. It also interacts with the backbone carbonyl of Glu377 (Fig. 4a). Water 84H mediates an interaction between the carboxylate group of the substrate and the active site residues Asp382, and partially with Arg388, Arg266, Tyr347 (for ∼500 ps). The electrostatic repulsion between the carboxylate groups of the active site residue Asp382 and the ligand is reduced by water mediation.

While water mediated interactions are prominent in the **1–iNOS** complex, the substrate in **1–eNOS** complex interacts directly with the active site residue Asn366. Additionally the **1–eNOS** complex is stabilized by a σ-bond cooperative chain, heme C═O···HO_wH (92H)···O_wH (168H)···O═C(**1**). Participation of water molecules in the molecular recognition of ligand within the active site is commonly found in several proteins [31–33]. However, in this context, water molecules seem to be critical in masking the active site differences, thereby facilitating the substrate binding in the NOS isoforms. The role of water is further confirmed by in silico mutation studies. The important residues have been mutated ((Asp382 in iNOS and Asn366 in eNOS to Asn382 and Asp366, respectively) to observe that water masks up these changes in the molecular recognition event (See supplementary data).

3.4. Mode of inhibitor binding in iNOS and eNOS isoforms

Replacement of the guanidinium nitrogen $N\eta_2$, required for the production of NO during the catalysis, with an amidino methyl carbon precludes molecule **2** from serving as substrate (Fig. 2). The methyl group sits snugly in the hydrophobic cavity formed by Gly371 (Gly355), Phe369 (Phe353), Val352 (Val337), and Pro350 (Pro335). Fig. 7 shows that the anchoring interactions between the amidino tail group of molecule **2** and that the carboxylate of Glu377 (Glu361) and Trp372 (Trp356) are retained in both isoforms. Molecule **2** contains an additional sulfone moiety that is placed in the hydrophobic cavity lined by

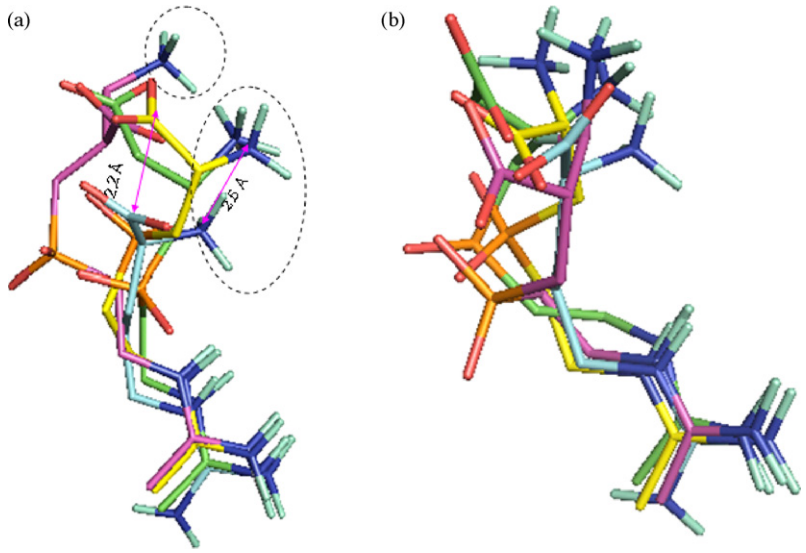

Fig. 8. Overlay of ligand conformations in (a) iNOS and (b) eNOS complexes. The C-atoms of the ligands are coloured as cyan (**1**); yellow (**2**); green (**3**); and pink (**4**). Distances between the ammonium and the carboxylic groups of substrate and molecule **2** are shown. Deviation of ammonium group of molecule **3** from that of molecules **1**–**4** can be seen (encircled).

Pro350 and Val352. Consequently, the ammonium group of molecule **2** gets displaced by 2.5 Å with respect to substrate (**1**) (Fig. 8). The displaced ammonium group in the **2–iNOS** complex therefore interacts directly with Asp382 and liberates the otherwise trapped water (82H) seen in the **1–iNOS** complex. Such an interaction is favourable in terms of entropy [34]. Also, the inclusion of sulfone shifts the contacts of the ammonium group from the side chain carboxylate to the backbone carbonyl of Glu377. Although the ligand does not interact with the heme carboxylate directly, the σ-bond cooperative chain mediates its interaction with heme and H_4B. Water 197H seems to be crucial in the **2–iNOS** complex as three σ-bond cooperative chains are mediated through it, namely (i) (**2**)HN···HO_w(196H)···HO_w(197H)···O=C(heme carboxylate); (ii) (**2**)HN···HO_w(196H)···HO_w(197H)···O12(H_4B)]; and (iii) (**2**)S=O···HO_wH (50H)···O_wH(197H)···O=C(H_4B). These interactions impart additional stability to the **2–iNOS** complex suggesting that because molecule **2** has a higher binding affinity to iNOS than the substrate (**1**) it acts as an inhibitor. Apart from these interactions, water 84H mediates interactions between carboxylate of **2** and the active site residues Tyr347, Asp382, Arg266, and Arg388.

In the **2–eNOS** complex, the ligand adopts an S-like conformation such that both the sulfone and carboxylate groups interact with Gln247 (Fig. 7b). Due to this conformational change, the ammonium group of the ligand gets displaced by about 2.3 Å, while the carboxylate group retains its position compared to the substrate in the **1–eNOS** complex (Fig. 8). The ammonium group therefore loses its interaction with Glu361 but interacts with heme and two water molecules, 1072w and 743w. Although the ammonium group interacts with water 743w throughout the simulation, no stable interactions are mediated to the protein residues. The carboxylate group interacts with Tyr357, Gln247, Arg250, Arg372, and Asn366. The **2–eNOS** complex is further stabilized by a σ-bond cooperative chain (**2**)NH···O_wH(1072w)···HO_w(168H)···HN(Arg365).

In comparison to iNOS, molecule **2** lacks one of the crucial interactions with the carbonyl O-atom of Glu361, a number of water mediated interactions (see occupancy Fig. 9) as well as the extra stabilization of the two σ-bond cooperative chains in

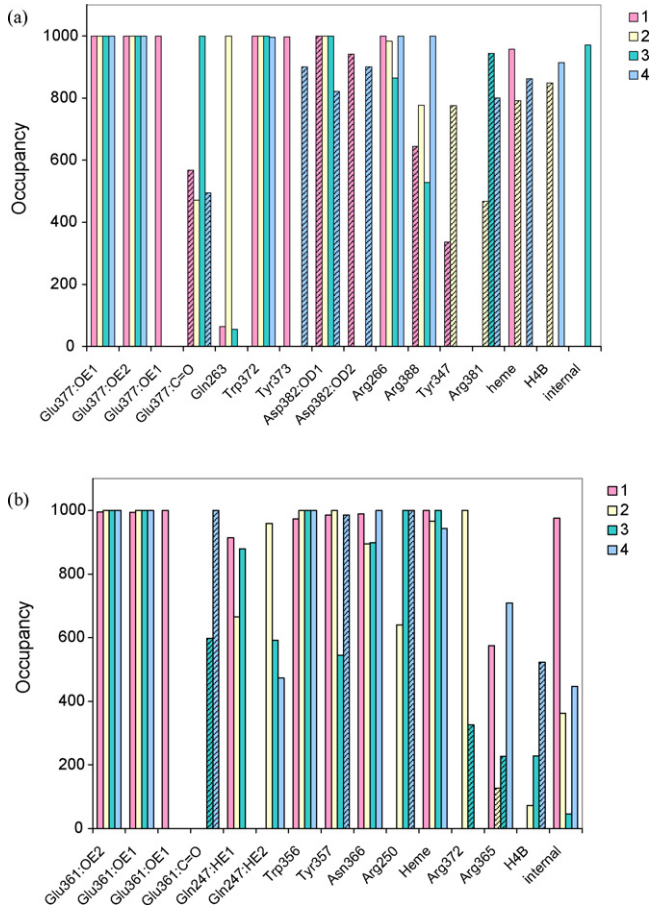

Fig. 9. Occupancy of the hydrogen bond interactions of ligands **1**–**4** in (a) iNOS and (b) eNOS complexes. Water mediated interactions are shaded.

eNOS. It has been suggested that σ-bond cooperative chains can contribute to the energy gain of around 20% relative to the isolated interactions [35]. Also, in the **2–iNOS** complex the methyl group of **2**, substituting for the guanidinium $N\eta_2$ of the substrate, is well placed in a hydrophobic cavity as mentioned earlier. In general, hydrophobic interactions have been postulated to contribute about 0.68 kcal mol^{-1} (or a 3.2-fold increase in binding constant) per methyl group to the binding energy [36]. However, such contributions have only been seen in the **2–iNOS** complex. In the **2–eNOS** complex, a water molecule, 556w is trapped in this hydrophobic cavity by interacting with the backbone carbonyl of Pro334, and backbone NH atoms of Phe353 and Gly355. The entropic penalty of trapping water 556w in the hydrophobic cavity could affect the stabilization energy of the **2–eNOS** complex. All the above interactions and differences contribute to higher selectivity of **2** towards iNOS when compared to eNOS. It is interesting to note that a water molecule bridging the carbonyl O-atom of Pro334 and the guanidine nitrogen of the substrate has been observed in the crystal structure of the eNOS–substrate complex [28]. Therefore, inclusion of 556w at this position is not either by chance or due to an artifact of the simulation, but that it has relevance to the structure of eNOS. However, the absence of such simulated water molecules in other isoforms complexes cannot be explained.

3.5. Rational design of more selective ligands

As observed with the interactions of ligands **1** and **2** in both the NOS isoforms, charge–charge interactions play a prominent role in the molecular recognition event. The juxtaposition of the positively and negatively charged groups in the ligand (α-amino acid head group) facilitates this molecular recognition, and (probably) selectivity among the isoforms. GRID analysis of the active sites of NOS isoforms also concurs that the hydrophobic and charge–charge interactions are the most important determinants of ligand selectivity [37]. We presume that selectivity can be improved by increasing the distance between the ammonium and the carboxylate groups. Accordingly, molecule **2** was modified to include a methylene spacer

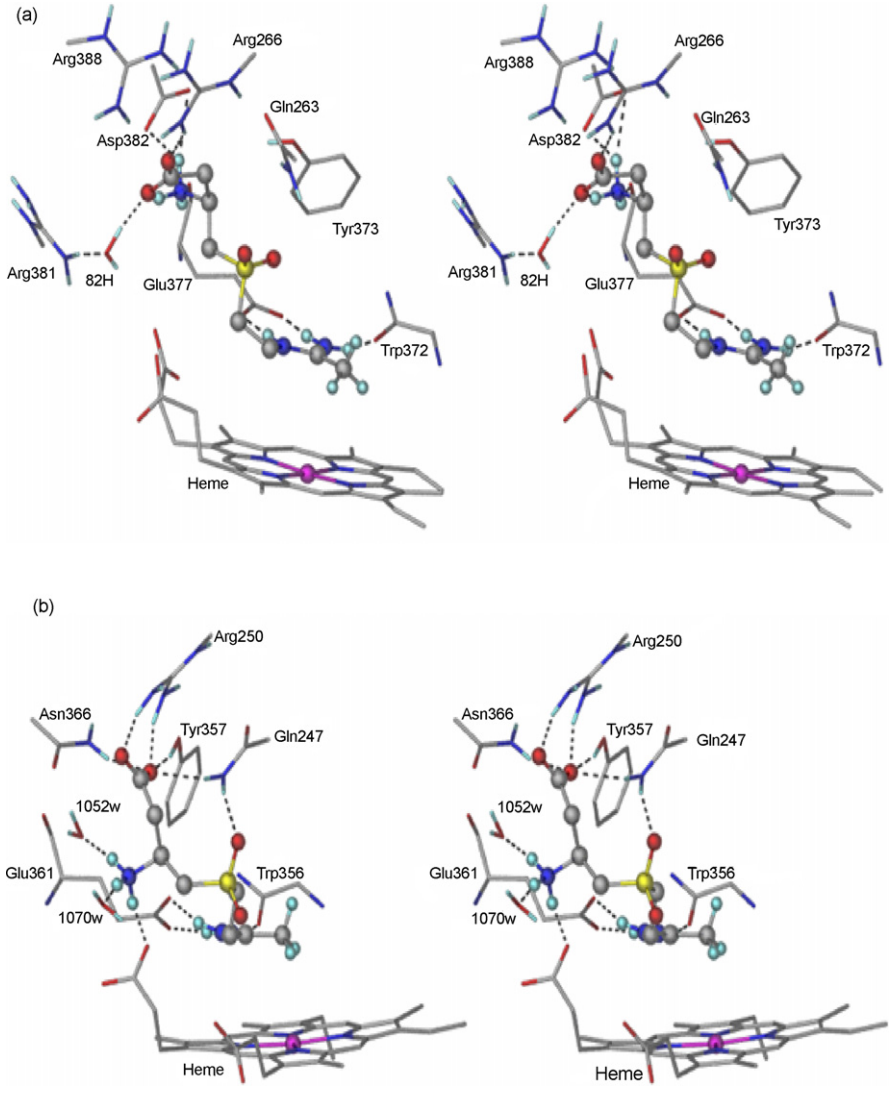

Fig. 10. Stereoview of the active site of the (a) **3–iNOS** and (b) **3–eNOS** complexes. Molecule **3** is shown in ball-and-stick.

between the oppositely charged groups. This resulted in two hypothetical ligands: **3**, wherein the methylene group was introduced between C_α atom and the carboxylate group and **4**, wherein the methylene was placed between the C_α atom and the ammonium group. Variations in the interactions of these modified ligands with both the isoforms are studied in detail and described in the following sections.

3.6. Mode of binding of molecule 3 in iNOS and eNOS

The interactions that anchor the ligand in the active site, namely the bidentate hydrogen bond between the amidino group of ligand and the carboxylate of Glu377 (Glu361) were retained in the complexes of **3** with both the isoforms. The RMSD between the bound conformations of molecule **3** in the two isoforms is 3.32 Å. In the **3–iNOS** complex, the spacer between the charged groups placed the functional groups such that they form an intramolecular hydrogen bond. The ammonium group of **3** interacts with the backbone carbonyl oxygen of Glu377 and the side chain carboxylate of Asp382 as shown in Fig. 10a. On the other hand introduction of an additional C-atom displaces the carboxylate group about 1.4 Å away from its initial position in molecule **2**. Consequently, the interaction with Gln263 is lost. A corresponding change in the RMSD of the residue Gln263 can be observed in Fig. 6. The carboxylate of the ligand interacts with Arg266. The occupancy plots of hydrogen bond interactions throughout the simulation shows that the interaction with Arg388 is retained for only ∼500 ps (Fig. 9). Apart from these, water (82H) mediated interactions were also observed between the ligand carboxylate and Arg381.

The interactions of the **3–eNOS** complex are shown in Fig. 10b. The ammonium group of **3** interacts with the heme carboxylate and two water molecules 1070w and 1052w. Water mediated (1052w) interactions are formed between the ammonium group and the backbone carbonyl of Glu361 (∼500 ps). However, no interactions are mediated through 1070w. Molecule **3** interacts with Gln247 through both its sulfone and the carboxylate groups, with a similar conformation as in the **2–eNOS** complex. Hydrogen bond interactions were also observed between the carboxylate group of **3** and the residues Asn366, Arg250 and partly with Tyr357 (∼500ps).

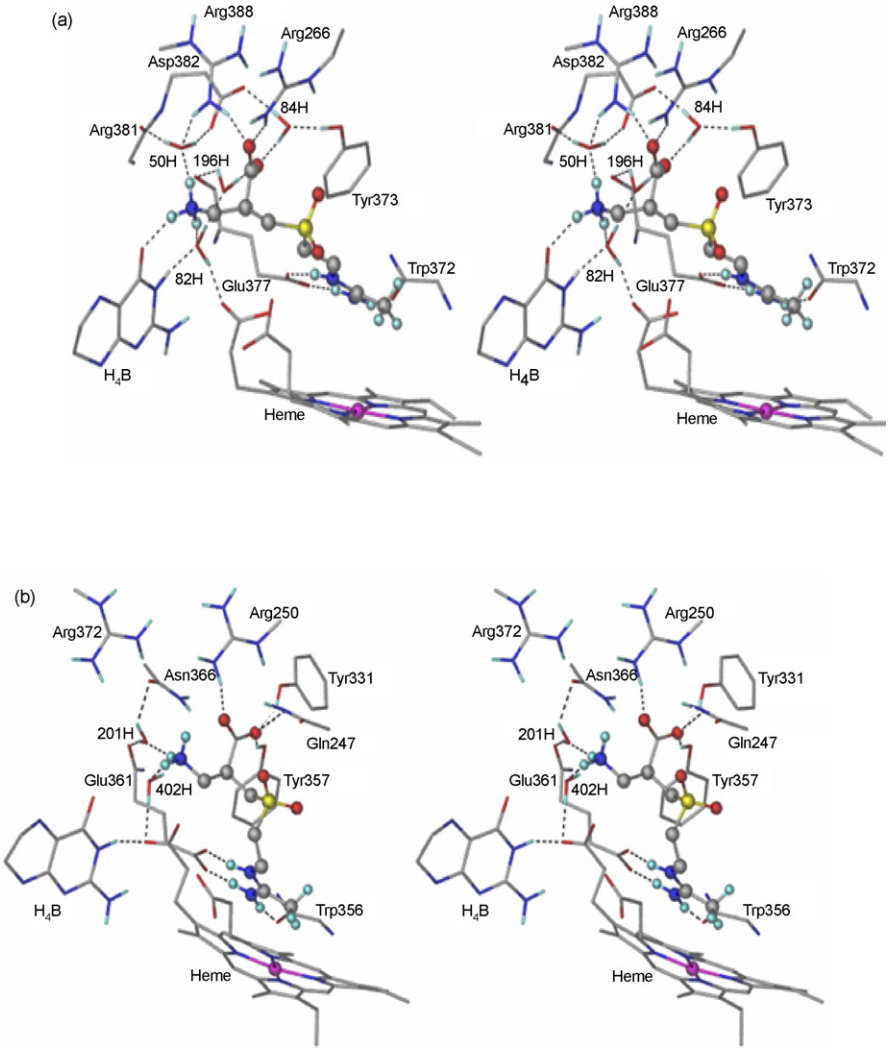

Fig. 11. Stereoview of the active site of the (a) **4–iNOS** and (b) **4–eNOS** complexes.

Although a few water molecules 107H, 757w and 1022w cluster around the sulfone moiety transiently, they do not form any interactions with the active site residues.

3.7. Mode of binding of molecule *4* in isoforms

The RMSD between the bound conformations of **4** in both the isoforms is 2.79 Å. Molecule **4** adopts a totally different conformation in iNOS when compared with other ligands in iNOS-complexes (Fig. 8a). The anchoring interactions in the active site remained unaltered in both the isoforms. In the **4–iNOS** complex, the ammonium group of **4** makes a direct interaction only with H_4B, while all the other interactions are mediated through water viz., 82H and 50H as shown in Fig. 11a. Hydrogen bond interactions with H_4B and heme were mediated through water 82H, while interactions with residues Asp382, Arg388, and Arg381 are through water 50H. Electrostatic interactions are seen between the carboxylate group of the ligand and the residues Arg388 and Arg266. The carboxylate group also forms water mediated interactions with Asp382 and Tyr373 residues through 84H and with Glu377 through 196H. Additionally, the **4–iNOS** complex was stabilized by the formation of σ-bond cooperative chain viz. (**4**) NH···O_wH(82H)···O_wH (196H)···O=C(Glu377).

In the **4–eNOS** complex, no direct interactions are formed with the ammonium group. Water mediated interactions with Asn366 and Glu361 through water 201H and with heme through water 402H are observed as shown in Fig. 11b. The ligand carboxylate interacts with Arg250 and Tyr357. The additional stability due to the σ-bond cooperative chain found in the **4–iNOS** complex was not found in the **4–eNOS** complex. Thus, a thorough inspection of these interactions predict molecule **4** to be a tighter binder to iNOS than to eNOS.

3.8. Comparison of binding of ligands in iNOS and eNOS

The occupancy plots of all the hydrogen bond interactions formed by the ligands **1–4** throughout the simulation in both iNOS and eNOS isoforms are shown in Fig. 9. All the interactions that persisted for a minimum of 500 ps duration were considered as being stable. Molecule **2** forms more number of interactions than molecule **1** with both isoforms. Also, molecule **2** forms more water mediated interactions in iNOS than in eNOS. This concurs with the experimental data that molecule **2** is more selective to iNOS than to eNOS [17]. As described above, such selectivity may be attributed to the presence of water mediated interactions and the extra stabilization of the σ-bond cooperative chains in the **2–iNOS** complex.

Molecule **3**, on the other hand, forms a smaller number of direct as well as water mediated interactions with both the isoforms. Therefore, incorporation of the methylene spacer between the C_α and the carboxylate as in molecule **3** does not improve the ligand binding to both isoforms. Upon a qualitative comparison of all the ligands binding to iNOS, molecule **4** is envisaged to have higher binding affinity with a maximum number of hydrogen bonds (6 direct interactions and 6 water mediated interactions), as each hydrogen bond contributes roughly to 3.5–5 kcal mol^{-1}. Also, when compared across the isoforms, molecule **4** forms a maximum number of stable interactions with iNOS than with eNOS indicating that it is deemed to bind more selectively to iNOS.

3.9. Energetics of ligand binding in iNOS and eNOS

The electrostatic and van der Waals contributions to the non-bonded interaction energies of ligands **1–4** forming direct interactions with active site residues in both iNOS are summarized in Table 3. From the interaction energies, it is evident that the active site residues Glu377, Trp372, Asp382, and heme have major contributions to the electrostatic energy in the ligand binding to iNOS. Molecule **2** has more favorable interaction energies with these residues when compared to other ligands **1** and **4**. Although molecule **3** showed much favorable electrostatic interaction energy with Asp382 (>6 kcal mol^{-1}), its interaction energy with heme was approximately 20 kcal mol^{-1} less than the other molecules.

Table 3
Non-bonded interaction energies of ligands **1–4** with iNOS (direct contacts)

Monomer	**1**		**2**		**3**		**4**	
	Coulomb	vdw	Coulomb	vdw	Coulomb	vdw	Coulomb	vdw
Gln263	0.36	−0.33	−7.28	0.23	2.28	−0.77	3.56	−0.75
Arg266	−1.25	1.85	−4.26	1.37	−3.27	1.42	−3.28	1.36
Pro350	−1.35	−0.96	−0.54	−1.00	−0.78	−1.02	−1.32	−1.02
Gly371	2.51	−0.17	3.57	−0.25	3.56	−0.31	3.76	−0.30
Trp372	−8.64	1.31	−11.61	1.39	−11.11	1.14	−11.43	0.77
Tyr373	0.54	−0.03	2.01	−0.82	5.04	−1.30	2.68	−1.02
Met374	0.86	−0.29	1.03	−0.18	2.54	−0.26	2.81	−0.13
Glu377	−69.17	4.77	−71.57	5.48	−78.69	6.87	−58.30	3.43
Arg381	1.87	0.76	17.35	−0.47	17.91	−0.49	4.95	−0.17
Asp382	−11.25	−0.26	−25.02	2.04	−31.35	1.52	−11.11	−0.38
Arg388	4.69	−0.07	9.30	0.24	11.76	0.16	6.30	0.86
Heme	−35.96	−2.82	−46.47	−4.24	−24.97	−4.37	−41.36	−3.61
H_4B	–	–	–	–	–	–	−4.27	0.50

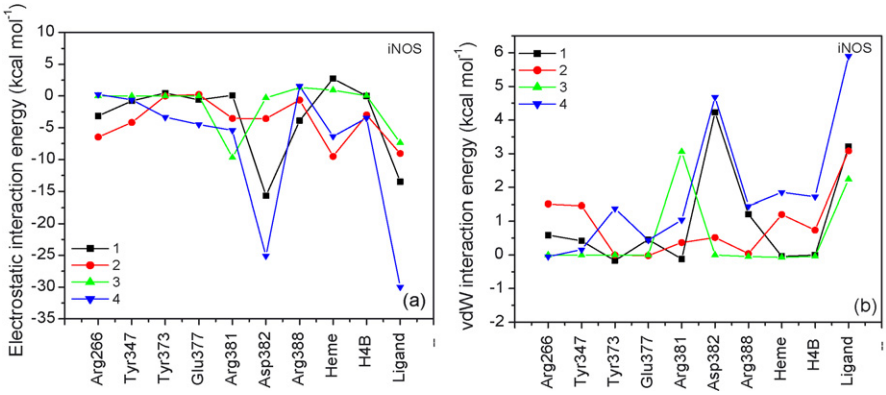

Fig. 12. (a) Electrostatic and (b) steric contributions to the non-bonded interaction energies of water mediated interactions in **1**–**4** iNOS complexes.

Table 4
Non-bonded interaction energies of ligands **1**–**4** with eNOS (direct contacts)

Monomer	**1**		**2**		**3**		**4**	
	Coulomb	vdw	Coulomb	vdw	Coulomb	vdw	Coulomb	vdw
Gln247	−0.25	0.02	−0.07	0.16	−1.49	0.35	−1.48	−0.52
Arg250	1.34	1.02	1.97	1.42	−4.61	2.65	−2.08	1.87
Pro334	0.09	−0.92	−1.46	−1.30	−0.50	−1.14	−1.17	−1.38
Gly355	4.21	−0.19	4.49	−0.30	−0.58	−0.24	2.67	−0.32
Trp356	−7.08	0.14	−8.83	1.42	−7.30	1.73	−7.28	1.28
Tyr357	0.76	−0.66	−1.22	1.08	2.46	−0.04	0.99	0.08
Met358	3.26	−0.31	1.49	−0.28	−20.85	−0.25	−5.65	−0.26
Glu361	−61.00	2.64	−64.41	4.79	−45.04	5.21	−57.87	3.45
Arg365	1.57	−0.02	2.59	−0.01	–	–	−0.35	−0.01
Asn366	−1.82	0.79	−3.84	−0.17	−0.87	0.76	−3.39	−0.24
Arg372	–	–	7.45	1.10	−0.16	0.59	0.73	–
Heme	−59.54	−1.21	−61.11	−2.52	−71.53	−1.56	−54.75	−4.17
H_4B	–	–	–	–	0.40	−0.06	0.21	−0.02

This favorable interaction energy may be directly related to higher binding affinity of molecule **2** towards iNOS. However, when the energies of water mediated interactions are taken into consideration (as shown in Fig. 12) molecule **4** is seen to have more favorable interaction energy with Glu377, Asp382, and heme. The plot shows that molecule **4** utilizes the active site variation of Asp382 in iNOS to a maximum extent, contributing about -30 kcal mol^{-1} to the electrostatic interaction energy. This concurs with the observation that molecule **4** forms maximum number of water mediated interactions as observed in Fig. 9. Although the van der Waals interactions have a destabilizing effect, they are compensated by the favorable electrostatic contributions. In comparison, molecule **2** although shows favorable interaction energy through direct interactions, molecule **4** surpasses this by forming water mediated interactions.

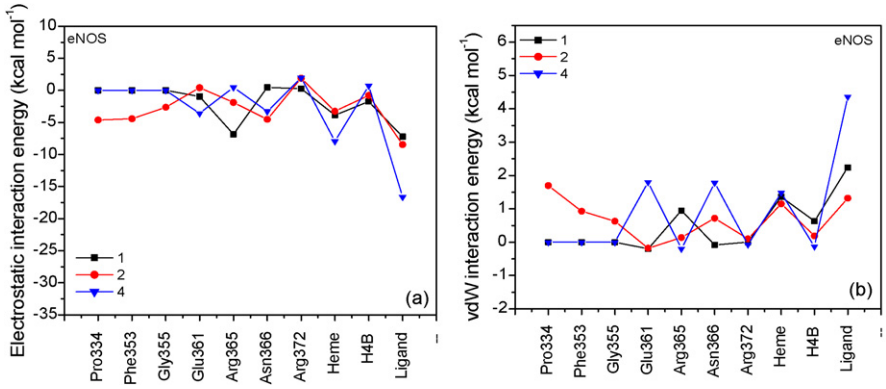

Fig. 13. (a) Electrostatic and (b) steric contributions to the non-bonded interaction energies of water mediated interactions in **1**–**4** eNOS complexes. Molecule **3** is not shown in figure as it has no water mediated interactions.

Table 4 shows the electrostatic and vdw interaction energies of ligands **1**–**4** forming direct interactions with the active site residues of eNOS. The table shows that molecule **2** and **4** have similar interaction energies as seen with the substrate, **1**. Fig. 13 shows the plot of water mediated interaction energies with active site residues of eNOS. No interactions were found to be water mediated in **3**–**eNOS** complex. Therefore, none of these molecules may have higher binding affinity compared to the substrate, **1**. Also, no major contributions were observed with the eNOS complexes indicating a minor role for water with eNOS compared to iNOS. Among all the ligand complexes, the energy contribution due to Asn366 (1–4 kcal mol^{-1}) in eNOS was far less than that due to Asp382 (10–30 kcal mol^{-1}) in iNOS. In summary, molecule **4** with more favorable water mediated interaction energies with iNOS may show higher selectivity to iNOS compared to eNOS.

4. Conclusions

Molecular dynamics simulations were performed for four ligand complexes with both iNOS and eNOS isoforms. MD simulations made it possible to identify and understand stable interactions in the enzyme–substrate/inhibitor complexes. The major difference in the substrate recognition among the isoforms is the interaction of the ammonium group of the substrate with Asp382 in iNOS that corresponds to Asn366 in eNOS. The substrate in the iNOS seems to have an entropic advantage over eNOS which could be speculated as a plausible reason for comparatively high turnover of the former. While the ammonium group forms a water mediated hydrogen bond in iNOS, the carboxylate group (of the substrate) interacts directly with the corresponding residue, Asn366 in eNOS. Analysis of the molecular recognition of the substrate in both the isoforms showed that water molecules seem to be critical in masking these active site differences, thereby, facilitating substrate binding. Especially, in iNOS, the electrostatic repulsion between the carboxylate groups of the substrate and Asp382 is reduced by water mediation. It is important to note that such repulsion is absent in the case of eNOS where the corresponding residue is Asn366. In eNOS, however, water has a different role to play of just providing hydrogen bonding groups in the active site.

MD simulations of an iNOS specific inhibitor **2** bound to both the isoforms indicates that in the **2**–**iNOS** complex the ammonium group interacts directly with Asp382 and liberates the otherwise trapped water seen in the **1**–**iNOS** complex. The basis of selectivity of molecule **2** towards iNOS was identified to be due to water mediated interactions and σ-bond cooperative networks. The juxtaposition of the positively and negatively charged groups in the ligand (α-amino acid head group) facilitates molecular recognition, and contributes to the selectivity differences in the various isoforms. The detailed analysis of both the substrate and the inhibitor recognition in the two isoforms provides useful guidelines for the design of potent isoform specific inhibitors. With a motto to explore the applications of MD to make structural variations and survey all possibilities, two hypothetical molecules **3** and **4** were designed by increasing the distance between the ammonium and the carboxylate groups of molecule **2**. The molecular recognition pattern of these ligands within the two isoforms was analyzed. Of the two, molecule **4** was envisaged to be more selective towards iNOS, based both on the number of interactions and the energetics involved therein. Water mediated interactions that remain stable throughout the simulations make a major contribution to the selectivity of molecule **4** to iNOS.

Acknowledgments

VA thanks the CSIR for fellowship support. GRD and AV acknowledge the Centre for Modelling, Simulation and Design (CMSD) set up in the University of Hyderabad under the UGC program for Universities with Potential for Excellence (UPE). We also thank the unknown reviewers for their comments and suggestions.

Appendix A. Supplementary data

Supplementary data associated with this article can be found, in the online version, at doi:10.1016/j.jmgm.2007.02.003.

References

[1] M.A. Marletta, Nitric oxide synthase: aspects concerning structure and catalysis, Cell 78 (1994) 927–930.
[2] H.W. Schmidt, U. Walter, NO at work, Cell 78 (1994) 919–925.
[3] H.M. Abu-Soud, D.J. Stuehr, Nitric oxide synthases reveal a role for calmodulin in controlling electron transfer, Proc. Natl. Acad. Sci. U.S.A. 90 (1993) 10769–10772.
[4] W.K. Alderton, C.E. Cooper, R.G. Knowles, Nitric oxide synthase: structure, function and inhibition, Biochem. J. 357 (2001) 593–615.
[5] V. Berka, H.C. Yeh, D. Gao, F. Kiran, A.L. Tsai, Redox function of tetrahydrobiopterin and effect of L-arginine on oxygen binding in endothelial nitric oxide synthase, Biochemistry 43 (2004) 13137–13148.
[6] M. Sørlie, A.F.C. Gorren, S. Marchal, T. Shimizu, R. Lange, K.K. Andersson, B. Mayer, Single-turnover of nitric-oxide synthase in the presence of 4-amino-tetrahydrobiopterin, J. Biol. Chem. 278 (2003) 48602–48610.
[7] A.R. Hurshman, C. Krebs, D.E. Edmondson, B.H. Huynh, M.A. Marletta, Formation of a pterin radical in the reaction of the heme domain of inducible nitric oxide synthase with oxygen, Biochemistry 38 (1999) 15689–15696.
[8] A. Messerschmidt, R. Huber, T. Poulos, K. Wieghardt, Inducible nitric oxide synthase, in: Handbook of Metalloproteins, John Wiley & Sons, Westsussex, 2001, pp. 285–299.
[9] W.M. Moore, R.K. Webber, G.M. Jerome, F.S. Tjoeng, T.P. Misko, M.G. Currie, L-N6-(1-Iminoethyl)lysine: a selective inhibitor of inducible nitric oxide synthase, J. Med. Chem. 37 (1994) 3886–3888.
[10] R.K. Webber, S. Metz, W.M. Moore, J.R. Connor, M.G. Currie, K.F. Fok, T.J. Hagen, D.W. Hansen Jr., G.M. Jerome, P.T. Manning, B.S. Pitzele, M.V. Toth, M. Trivedi, M.E. Zupec, F.S. Tjoeng, Substituted 2-iminopiperidines as inhibitors of human nitric oxide synthase isoforms, J. Med. Chem. 41 (1998) 96–101.
[11] H. Matter, P. Kotsonis, Biology and chemistry of the inhibition of nitric oxide synthases by pteridine- derivatives as therapeutic agents, Med. Res. Rev. 24 (2004) 662–684.
[12] B.R. Crane, A.S. Arvai, A.R. Gachhui, C. Wu, D.K. Ghosh, E.D. Getzoff, D.J. Steuhr, J.A. Tainer, The structure of nitric oxide synthase oxygenase domain and inhibitor complexes, Science 278 (1997) 425–438.
[13] B.R. Crane, A.S. Arvai, D.K. Ghosh, C. Wu, E.D. Getzoff, D.J. Stuehr, J.A. Tainer, Structure of nitric oxide synthase oxygenase dimer with pterin and substrate, Science 279 (1998) 2121–2126.

[14] R. Federov, R. Vasan, D.K. Ghosh, I. Schlichthing, Structures of nitric oxide synthase isoforms complexed with the inhibitor AR-R17477 suggest a rational basis for specificity and inhibitor design, Proc. Natl. Acad. Sci. U.S.A. 101 (2004) 5892–5897.
[15] T.O. Fischmann, A. Hruza, X.D. Niu, J.D. Fossetta, C.A. Lunn, E. Dolphin, A.J. Prongay, P. Reichert, D.J. Lundell, S.K. Narula, P.C. Weber, Structural characterization of nitric oxide synthase isoforms reveals striking active-site conservation, Nat. Struct. Biol. 6 (1999) 233–242.
[16] C.S. Raman, H. Li, P. Martasek, B.R. Babu, O.W. Griffith, B.S.S. Masters, T.L. Poulos, Implications for isoform selective inhibitor design derived from the binding mode of bulky isothioureas to the heme domain of endothelial nitric oxide synthase, J. Biol. Chem. 276 (2001) 26486–26491.
[17] R.J. Young, R.M. Beams, C. Keith, H.A.R. Clark, D.M. Coe, C.L. Chambers, P.I. Davies, J. Dawson, M.J. Drysdale, W. Karl, K.W. Franzman, C. French, S.T. Hodgson, H.F. Hodson, S. Kleanthous, P. Rider, D. Sanders, D.A. Sawyer, K.J. Scott, B.G. Shearer, R. Stocker, S. Smith, M.C. Tackley, R.G. Knowles, Inhibition of inducible nitric oxide synthase by acetamidine derivatives of hetero-substituted lysine and homolysine, Bioorg. Med. Chem. Lett. 10 (2000) 597–600.
[18] H. Li, C.S. Raman, C.B. Glaser, E. Blasko, A. Tish, T.A. Young, F. John, J.F. Parkinsoni, M. Whitlow, T.L. Poulos, Crystal structures of Zinc-free and -bound heme domain of human inducible nitric-oxide synthase, J. Biol. Chem. 274 (1999) 21276–21284.
[19] InsightII, Version 2005, Accelrys, San Diego, CA.
[20] S. Shi, L. Yan, Y. Yang, J. Fisher-shaulsky, T. Thacher, An extensible and systematic force field, ESFF, for molecular modeling of organic, inorganic, and organometallic systems, J. Comput. Chem. 24 (2003) 1059–1076.
[21] Cerius^2, Version 4.8, Accelrys, San Diego, CA.
[22] GOLD, Version 3.1, Cambridge Crystallographic Data Centre, Cambridge, UK.
[23] T.L. Poulos, Structural and functional diversity in heme monooxygenases, Drug Metab. Dispos. 33 (2005) 10–18.
[24] W.L. Jorgensen, J. Chandrasekhar, J.D. Madura, R.W. Impey, M.L. Klein, Comparison of simple potential function for simulating liquid water, J. Chem. Phys. 79 (1983) 926–935.
[25] G.J. Martyna, M.L. Klein, M. Tuckerman, Nosé-Hoover chains: the canonical ensemble via continuous dynamics, J. Chem. Phys. 97 (1992) 2635–2643.
[26] P. Chen, A. Tsai, V. Berka, K.K. Wu, Mutation of Glu-361 in human endothelial nitric-oxide synthase selectively abolishes L-arginine binding without perturbing the behavior of heme and other redox centers, J. Biol. Chem. 272 (1997) 6114–6118.
[27] O.W. Griffith, D.J. Stuehr, Nitric oxide synthases: properties and catalytic mechanism, Annu. Rev. Physiol. 57 (1995) 707–736.
[28] H. Li, C.S. Raman, P. Martásek, B.S.S. Masters, T.L. Poulos, Crystallographic studies on endothelial nitric oxide synthase complexed with nitric oxide and mechanism-based inhibitors, Biochemistry 40 (2001) 5399–5406.
[29] S.K. Grant, B.G. Green, J. Stiffey-Wilusz, P.L. Durette, S.K. Shah, J.W. Kozarich, Structural requirements for human inducible nitric oxide synthase substrates and substrate analogue inhibitors, Biochemistry 37 (1998) 4174–4180.
[30] J.E. Ladbury, Just add water! the effect of water on the specificity of protein-ligand binding sites and its potential application to drug design, Chem. Biol. 3 (1996) 973–980.
[31] B.S. Sanjeev, S. Vishveshwara, Dynamics of the native and the ligand-bound structures of eosinophil cationic protein: network of hydrogen bonds at the catalytic site, J. Biomol. Struct. Dyn. 22 (2005) 657–672.
[32] S. Sarkhel, G.R. Desiraju, N–H···O, O–H···O, and C–H···O hydrogen bonds in protein–ligand complexes: strong and weak interactions in molecular recognition, Proteins 54 (2004) 247–259.
[33] B. Gopalakrishnan, V. Aparna, J. Jeevan, M. Ravi, G.R. Desiraju, A Virtual screening approach for thymidine monophosphate kinase inhibitors as antitubercular agents based on docking and pharmacophore models, J. Chem. Inf. Model. 45 (2005) 1101–1108.
[34] J.D. Dunitz, The entropic cost of bound water in crystals and biomolecules, Science 264 (1994) 670.
[35] S. Scheiner, Hydrogen Bonding: A Theoretical Perspective, Oxford University Press, Oxford, 1997.
[36] A.M. Davis, S.J. Teague, Hydrogen bonding, hydrophobic interactions, and failure of the rigid receptor hypothesis, Angew. Chem. Int. Ed. 38 (1999) 736–749.
[37] H. Ji, H. Li, M. Flinspach, T.L. Poulos, R.B. Silverman, Computer modeling of selective regions in the active site of nitric oxide synthase: implication for the design of isoform-selective inhibitors, J. Med. Chem. 46 (2003) 5700–5711.